

DISCOVERY OF A BINARY BROWN DWARF AT 2 PARSECS FROM THE SUN<sup>1</sup>K. L. LUHMAN<sup>2,3</sup>*Draft version March 4, 2019*

## ABSTRACT

I am using multi-epoch astrometry from the *Wide-field Infrared Survey Explorer (WISE)* to search for new members of the solar neighborhood via their high proper motions. Through this work, I have identified WISE J104915.57-531906.1 as a high proper motion object and have found additional detections in images from the Digitized Sky Survey, the Two Micron All-Sky Survey, and the Deep Near-Infrared Survey of the Southern Sky. I have measured a parallax of  $0.496 \pm 0.037''$  ( $2.0 \pm 0.15$  pc) from the astrometry in these surveys, making WISE J104915.57-531906.1 the third closest system to the Sun. During spectroscopic observations with GMOS at Gemini Observatory, an *i*-band acquisition image resolved it as a  $1''.5$  (3 AU) binary. A spectrum was collected for the primary, which I classify as  $L8 \pm 1$ . The secondary is probably near the L/T transition as well given that it is only modestly fainter than the primary ( $\Delta i = 0.45$  mag).

*Subject headings:* brown dwarfs — infrared: stars — proper motions — solar neighborhood — stars: low-mass

## 1. INTRODUCTION

Stars in the solar neighborhood have been identified primarily through their large proper motions (e.g., Barnard 1916; Wolf 1919; Ross 1926; van Biesbroeck 1944; Giclas et al. 1971; Luyten 1979; Lépine & Shara 2005). Most brown dwarfs, on the other hand, have been found through their distinctive colors (e.g., Burgasser et al. 2004; Cruz et al. 2007; Burningham et al. 2010; Albert et al. 2011; Kirkpatrick et al. 2011) because wide-field infrared (IR) surveys initially offered limited data on proper motions. However, a significant amount of multi-epoch astrometry is now available from various combinations of the Two Micron All-Sky Survey (2MASS, Skrutskie et al. 2006), the Deep Near-Infrared Survey of the Southern Sky (DENIS, Epchtein et al. 1999), the Sloan Digital Sky Survey (SDSS, York et al. 2000), the United Kingdom Infrared Telescope Infrared Deep Sky Survey (UKIDSS, Lawrence et al. 2007), Pan-STARRS1 (PS1, Kaiser et al. 2002), and the survey performed by the *Wide-field Infrared Survey Explorer (WISE)*, Wright et al. 2010). As a result, the role of proper motions in brown dwarf searches is expanding rapidly (Sheppard & Cushing 2009; Artigau et al. 2010; Kirkpatrick et al. 2010; Deacon et al. 2009, 2011; Liu et al. 2011; Gizis et al. 2011; Scholz et al. 2011, 2012).

The *WISE* satellite imaged each position in the sky at multiple epochs that span 6–12 months, which enables proper motion measurements with *WISE* data alone. The accuracy of *WISE* astrometry ( $0''.2$  at  $\text{SNR} > 50$ ) is lower than that of other modern wide-field surveys, but it

provides the best sensitivity to the coolest brown dwarfs (Cushing et al. 2011). In addition, it is easier to detect the highest proper motions exhibited by stars ( $\mu \sim 1\text{--}10'' \text{ yr}^{-1}$ ) through multiple identical mappings across a baseline of less than a year than with a comparison of surveys conducted at different wavelengths and at more widely separated epochs. Through an analysis of the multi-epoch astrometry from *WISE*, I have discovered one the closest neighbors of the Sun, which I present in this Letter.

2. PROPER MOTION SURVEY WITH *WISE*

*WISE* was designed to complete a map of the entire sky in 6 months. Given that its mission lifetime was nearly 13 months, it was able to perform two full surveys of the sky and begin a third one. In each 6 month survey, *WISE* obtained one 8.8 sec exposure in each operable band every 1.5 hours for a period ranging from 12 hours near the ecliptic plane to 6 months at the ecliptic poles. The four bands of *WISE* were centered at 3.4, 4.6, 12, and 22  $\mu\text{m}$ , which are denoted as *W1*, *W2*, *W3*, and *W4*, respectively. All of the bands were employed from 2010 January 7 through 2010 August 6. Because of the successive exhaustion of the outer and inner cryogen tanks, images were not collected through *W4* and *W3* after 2010 August 6 and 2010 September 29, respectively. The satellite continued to observe in *W1* and *W2* until 2011 February 1 (Mainzer et al. 2011).

To search for high proper motion objects with *WISE*, I began by retrieving astrometry and photometry from the All-Sky Single Exposure (L1b) Source Table, the 3-Band Cryo Single Exposure (L1b) Source Table, and the Preliminary Post-Cryo Single Exposure (L1b) Source Table for all sources that lacked 2MASS counterparts within  $3''$ . I chose to omit sources with close 2MASS counterparts to focus my search on objects with either high proper motions ( $\mu \gtrsim 0''.3 \text{ yr}^{-1}$ ) or low temperatures ( $\gtrsim T7$  at 10 pc). Using TOPCAT<sup>4</sup> and STILTS<sup>5</sup> (Taylor 2005,

<sup>1</sup> Based on data from the *Wide-field Infrared Survey Explorer*, Gemini Observatory, the Two Micron All-Sky Survey, the Deep Near-Infrared Survey of the Southern Sky, and the Digitized Sky Survey.

<sup>2</sup> Department of Astronomy and Astrophysics, The Pennsylvania State University, University Park, PA 16802, USA; kluhman@astro.psu.edu

<sup>3</sup> Center for Exoplanets and Habitable Worlds, The Pennsylvania State University, University Park, PA 16802, USA

<sup>4</sup> <http://www.starlink.ac.uk/topcat/>

<sup>5</sup> <http://www.starlink.ac.uk/stilts/>

2006), I identified all groups of detections that had separations of  $< 1''.5$  and  $< 1$  day between neighboring detections. Thus, these groups were designed to contain all detections of a source during the time that it was observed continuously. Each of these periods is referred to as an “epoch” in the remaining discussion.

Using the average coordinates of detections within a given epoch, I matched sources from different epochs, computed the proper motions ( $\mu$ ) for these matches, and identified the matches with  $\mu/\sigma_\mu > 3$ . Among the resulting high proper motion candidates, I omitted those that have been found in previous studies and that appeared extended or blended with other sources upon visual inspection. Nearly all of the remaining candidates that were detected in  $W3$  and  $W4$  exhibited very red colors that were indicative of galaxies ( $W2 - W3 > 2$ ,  $W3 - W4 > 1.5$ ), and thus their putative motions were likely caused by resolved emission. However, one of these candidates was only modestly red, and hence closer to the colors observed for stellar sources. This candidate corresponds to WISE J104915.57–531906.1 (hereafter WISE 1049–5319) and consisted of 12, 19, and 18 detections near 2010 January 9, 2010 July 2, and 2011 January 6, respectively. I inspected images from 2MASS, DENIS, and the Digitized Sky Survey (DSS) at the positions expected for WISE 1049–5319 given the proper motion measured from the three *WISE* epochs. It is detected at  $J$ ,  $H$ , and  $K_s$  ( $1.25, 1.65, 2.16 \mu\text{m}$ ) with 2MASS and at  $i$  ( $0.8 \mu\text{m}$ ),  $J$ , and  $K_s$  with DENIS. It appears in the red and IR ( $0.66, 0.85 \mu\text{m}$ ) images of DSS, but not the blue image ( $0.45 \mu\text{m}$ ). The detections of WISE 1049–5319 in DSS IR and red, 2MASS  $J$ , DENIS  $J$ , and *WISE*  $W1$  are shown in Figure 1. I also include the  $i$ -band acquisition image obtained during spectroscopic observations of WISE 1049–5319 (Section 3.1). The *WISE* image is displayed on a logarithmic scale so that sources near the detection limit can be seen while keeping WISE 1049–5319 relatively unsaturated.

### 3. CHARACTERIZATION OF WISE 1049–5319

#### 3.1. Photometric and Spectroscopic Properties

To investigate the photometric properties of WISE 1049–5319, I have plotted it on color-magnitude and color-color diagrams in Figure 3 that are constructed from 2MASS and *WISE* bands. The absolute magnitude in  $W2$  is computed with the parallax measured in Section 3.2. For comparison, I have included a sample of known M, L, and T dwarfs (Leggett et al. 2010; Kirkpatrick et al. 2011, 2012, <http://DwarfArchives.org>). 2MASS measurements are shown for these field dwarfs since the near-IR data for WISE 1049–5319 are also from 2MASS. All of the data for WISE 1049–5319 in Figure 3 are consistent with a dwarf between spectral types of  $\sim\text{L5}$  and  $\text{L9}$ . The position of WISE 1049–5319 in  $M_{W2}$  versus  $W1 - W2$  and is modestly brighter than the lower envelope of the L dwarf sequence, which is suggestive of an unresolved binary. A similar offset is present in various other IR color-magnitude diagrams as well. Finally, I note that the entry for WISE 1049–5319 in the All-Sky Source Catalog, which consists of the 31 detections from the first two epochs, is flagged as a possible variable in  $W1$  and  $W2$ . Thus, it may be an attractive target for de-

tailed photometric monitoring (e.g., Artigau et al. 2009; Radigan et al. 2012).

To measure the spectral type of WISE 1049–5319, I pursued spectroscopy of it with the Gemini Multi-Object Spectrograph (GMOS) at the Gemini South telescope on the night of 2013 February 23. The observations began with a 10 s  $i$ -band exposure for target acquisition. The FWHM of point sources in this image was  $0''.6$ . At the position expected for WISE 1049–5319 given its proper motion, a  $1''.5$  pair with  $\Delta i = 0.45$  mag was detected. I conclude that both objects are counterparts to WISE 1049–5319 and that they comprise a binary system since the images from DSS, DENIS, and 2MASS do not detect a source at that location. The binarity of WISE 1049–5319 is consistent with its overluminous position in Figure 3. Spectroscopy was performed on the brighter (southeast) component, which I refer to as WISE 1049–5319 A. The spectrograph was configured with the 400 l/mm grating, the RG610 order blocking filter, and the  $0''.75$  slit, which produced data with a resolution of  $5 \text{ \AA}$ . The slit was aligned to the parallactic angle and two 5 min exposures were collected. The resulting spectrum is shown in Figure 4. It matches closely with the spectrum of the L8 dwarf standard 2MASS J16322911+1904407 from Kirkpatrick et al. (1999). Based on a comparison to the other standards from that study, the uncertainty in this classification is  $\pm 1$  subclass. The hydrogen burning limit is predicted to occur at  $T_{\text{eff}} \gtrsim 1700 \text{ K}$  (Chabrier & Baraffe 2000; Burrows et al. 2001) for ages less than 10 Gyr, which corresponds to spectral types of  $\lesssim\text{L5}$  (Golimowski et al. 2004). Thus, WISE 1049–5319 A is very likely a brown dwarf. The presence of strong lithium absorption ( $W_\lambda = 8 \pm 1 \text{ \AA}$ ) provides further support for its substellar nature (Rebolo et al. 1992). Given the flux ratio of the pair, the secondary is probably a brown dwarf as well with a spectral type of late L or early T.

#### 3.2. Parallax and Proper Motion

The binarity of WISE 1049–5319 has implications for the measurement of its parallax and proper motion. In an unresolved binary containing unequal components, the orbital motion is reflected in movement of the photocenter, which can introduce errors into derived parallax and proper motion (e.g., Dupuy & Liu 2012). In the case of WISE 1049–5319, its separation and the substellar masses of its components are indicative of an orbital period of  $\sim 25$  years. Since this is much longer than the baseline of one year across which parallactic motion occurs, the measurement of parallax should be unaffected. Because the astrometry for WISE 1049–5319 spans a timescale of decades, the measured proper motion is more susceptible to an error from the motion of the photocenter, but the effect is still quite small. For instance, using the  $i$ -band flux ratio, the amplitude of the shift of the photocenter is only  $\sim 0.5\%$  of the total motion of WISE 1049–5319 over the period for which astrometry is available. However, if the flux ratio of a system varies with wavelength, then the position of the photocenter will do so as well, which can lead to errors in both the proper motion and parallax if they are based on multi-wavelength astrometry. To mitigate such errors, I have excluded the

GMOS astrometry from the measurement of the parallax and proper motion. The other astrometric data are either from IR bands (*WISE*, DENIS, 2MASS), within which the flux ratio should not vary as much as in the optical, or already have uncertainties that are larger than this effect. Focusing on the IR astrometry offers an additional advantage; because optical-to-IR colors of L and T dwarfs become redder with later types, the flux ratio of WISE 1049–5319 is probably closer to unity at IR wavelengths than that measured with GMOS in the *i* band, corresponding to a smaller motion of the photocenter.

I adopted the astrometry from the 2MASS Point Source Catalog and the Third DENIS Release. For each *WISE* epoch, I computed the mean of the coordinates that were retrieved from the single-exposure catalogs, with the exception of one detection from the second epoch with discrepant coordinates. For the DSS images, I measured the positions of the counterpart to WISE 1049–5319 with the IRAF task *starfind*. The counterparts in 2MASS and DENIS are partially blended with a star at a distance of  $\sim 3''$  to the north. The latter should be  $\sim 5$  mag fainter than WISE 1049–5319 in the near-IR bands of 2MASS and DENIS based on its optical photometry from the USNO-B1.0 Catalog (Monet et al. 2003). Thus, the astrometry from the 2MASS and DENIS should be negligibly affected by the fainter star. To place all astrometry on the same reference system, I computed the average offset in right ascension and declination between 2MASS and the other surveys for sources within a few arcminutes of WISE 1049–5319. These offsets were then applied to the coordinates for WISE 1049–5319 from DSS, DENIS, and each of the *WISE* epochs to align them to the 2MASS system.

For the *WISE* astrometric errors, I adopted the standard deviations of the right ascensions and declinations of the individual detections at a given epoch. For 2MASS, I adopted the errors from the Point Source Catalog. To estimate the errors for DSS and DENIS, I assumed that their sum in quadrature with the errors from the 2MASS equaled the standard deviations of the differences in right ascension and declination between DSS/2MASS and DENIS/2MASS for stars near the flux of WISE 1049–5319. The detection in DSS IR is partially blended with a fainter source to the east. In an attempt to account for the effect on the astrometry, I doubled the error for its astrometry. The astrometry for WISE 1049–5319 from DSS, 2MASS, DENIS, and *WISE* is compiled in Table 1.

I have performed least-squares fitting of proper and parallactic motion to the astrometry for WISE 1049–5319 using the IDL program MPFIT. The resulting measurements of the parallax and proper motion are presented in Table 2. The parallax corresponds to a distance of  $2.0 \pm 0.15$  pc. To test the validity of the errors, I fitted 1000 sets of astrometry that were generated by adding Gaussian noise to the measured positions. The standard deviations of the resulting values of parallax and proper motion agreed with the uncertainties produced by MPFIT. In Figure 2, the measured astrometric offsets after removal of proper motion are plotted with the offsets are expected for the derived value of the parallax. Although the DSS data have large uncertainties, they do provide tight constraints on the proper motion because of the long baseline, which in turn allows the

2MASS and *WISE* data to better constrain the parallax.

#### 4. DISCUSSION

With a distance of  $2.0 \pm 0.15$  pc, WISE 1049–5319 is the closest neighbor of the Sun that has been found in nearly a century (Henderson 1839; Barnard 1916; Adams & Joy 1917; Voûte 1917). It is only slightly more distant than Barnard’s star, which is the second nearest known system ( $1.834 \pm 0.001$  pc, Benedict et al. 1999). The low galactic latitude of WISE 1049–5319 ( $l = 5^\circ$ ) is likely the reason why it was not found in previous surveys for nearby brown dwarfs, which have tended to avoid the galactic plane. Because of its proximity to the Sun, WISE 1049–5319 is a unique target for a variety of studies, such as direct imaging and radial velocity searches for planets.

I acknowledge support from grant NNX12AI47G from the NASA Astrophysics Data Analysis Program. *WISE* is a joint project of the University of California, Los Angeles, and the Jet Propulsion Laboratory (JPL)/California Institute of Technology (Caltech), funded by NASA. The Gemini data were obtained through program GN-2013A-DD-2. Gemini Observatory is operated by the Association of Universities for Research in Astronomy, Inc., under a cooperative agreement with the NSF on behalf of the Gemini partnership: the National Science Foundation (United States), the National Research Council (Canada), CONICYT (Chile), the Australian Research Council (Australia), Ministério da Ciência, Tecnologia e Inovação (Brazil) and Ministerio de Ciencia, Tecnología e Innovación Productiva (Argentina). 2MASS is a joint project of the University of Massachusetts and the Infrared Processing and Analysis Center (IPAC) at Caltech, funded by NASA and the NSF. The Digitized Sky Survey was produced at the Space Telescope Science Institute under U.S. Government grant NAG W-2166. The images of these surveys are based on photographic data obtained using the Oschin Schmidt Telescope on Palomar Mountain and the UK Schmidt Telescope. The plates were processed into the present compressed digital form with the permission of these institutions. This work uses data from the M, L, and T dwarf compendium at <http://DwarfArchives.org> (maintained by Chris Gelino, Davy Kirkpatrick, and Adam Burgasser) and the NASA/IPAC Infrared Science Archive (operated by JPL under contract with NASA). The Center for Exoplanets and Habitable Worlds is supported by the Pennsylvania State University, the Eberly College of Science, and the Pennsylvania Space Grant Consortium. The DENIS project was partly funded by the SCIENCE and the HCM plans of the European Commission under grants CT920791 and CT940627. It was supported by INSU, MEN and CNRS in France, by the State of Baden-Württemberg in Germany, by DGICYT in Spain, by CNR in Italy, by FFwFBWF in Austria, by FAPESP in Brazil, by OTKA grants F-4239 and F-013990 in Hungary, and by the ESO C&EE grant A-04-046. Jean Claude Renault from IAP was the Project manager. Observations were carried out thanks to the contribution of numerous students and young scientists from all involved institutes, under the supervision of P. Fouqué.

## REFERENCES

- Adams, W. S., & Joy, A. H. 1917, *ApJ*, 46, 313
- Albert, L., Étienne, A., Delorme, P., et al. 2011, *AJ*, 141, 203
- Artigau, É., Bouchard, S., Doyon, R., & Lafrenière, D. 2009, *ApJ*, 701, 1534
- Artigau, É., Radigan, J., Folkes, S., et al. 2010, *ApJ*, 718, L38
- Barnard, E. E. 1916, *AJ*, 29, 191
- Benedict, G. F., McArthur, B., Chappell, D. W., et al. 1999, *AJ*, 118, 1086
- Burgasser, A. J., McElwain, M. W., Kirkpatrick, J. D., et al. 2004, *AJ*, 127, 2856
- Burningham, B., Pinfield, D. J., Lucas, P. W., et al. 2010, *MNRAS*, 406, 1885
- Burrows, A., Hubbard, W. B., Lunine, J. I., & Liebert, J. 2001, *Rev. Mod. Phys.*, 73, 719
- Chabrier, G., & Baraffe, I. 2000, *ARA&A*, 38, 337
- Cruz, K. L., Reid, I. N., Kirkpatrick, J. D., et al. 2007, *AJ*, 133, 439
- Cushing, M. C., Kirkpatrick, J. D., Gelino, C. R., et al. 2011, *ApJ*, 743, 50
- Deacon, N. R., Hambly, N. C., King, R. R., & McCaughrean, M. J. 2009, *MNRAS*, 394, 857
- Deacon, N. R., Liu, M. C., Magnier, E. A., et al. 2011, *AJ*, 142, 77
- Dupuy, T. J., & Liu, M. C. 2012, *ApJS*, 201, 19
- Epchtein, N., Deul, E., Derriere, S., et al. 1999, *A&A*, 349, 236
- Giclas, H. L., Burnham, R., & Thomas, N. G. 1971, *The Lowell Proper Motion Survey* (Flagstaff, AZ: Lowell Observatory)
- Gizis, J. E., Troup, N. W., & Burgasser, A. J. 2011, *ApJ*, 736, L34
- Golimowski, D. A., Leggett, S. K., Marley, M. S., et al. 2004, *AJ*, 127, 3516
- Henderson, T. 1839, *MNRAS*, 4, 168
- Kaiser, N., Aussel, H., Burke, B. E., et al. 2002, *Proc. SPIE*, 4836, 154
- Kirkpatrick, J. D., Cushing, M. C., Gelino, C. R., et al. 2011, *ApJS*, 197, 19
- Kirkpatrick, J. D., Gelino, C. R., Cushing, M. C., et al. 2012, *ApJ*, 753, 156
- Kirkpatrick, J. D., Looper, D. L., Burgasser, A. J., et al. 2010, *ApJS*, 190, 100
- Kirkpatrick, J. D., Reid, I. N., Liebert, J., et al. 1999, *ApJ*, 519, 802
- Lawrence, A., Warren, S. J., Almaini, O., et al. 2007, *MNRAS*, 379, 1599
- Leggett, S. K., Burningham, B., Saumon, D., et al. 2010, *ApJ*, 710, 1627
- Lépine, S., & Shara, M. M. 2005, *AJ*, 129, 1483
- Liu, M. C., Deacon, N. R., Magnier, E. A., et al. 2011, *ApJ*, 740, L32
- Luyten, W. J. LHS Catalogue. A Catalogue of Stars with Proper Motions Exceeding 0"5 annually, 2nd edn. Univ. Minnesota, Minneapolis, MN
- Mainzer, A., Bauer, J., Grav, T., et al. 2011, *ApJ*, 731, 53
- Monet, D. G., Levine, S. E., Canzian, B., et al. 2003, *AJ*, 125, 984
- Radigan, J., Jayawardhana, R., Lafrenière, D., et al. 2012, *ApJ*, 750, 105
- Rebolo, R., Martín, E. L., & Magazzù, A. 1992, *ApJ*, 389, L83
- Ross, F. E. 1926, *AJ*, 36, 124
- Scholz, R.-D., Bihain, G., Schnurr, O., & Storm, J. 2011, *A&A*, 532, L5
- Scholz, R.-D., Bihain, G., Schnurr, O., & Storm, J. 2012, *A&A*, 541, A163
- Sheppard, S. S., & Cushing, M. C. 2009, *AJ*, 137, 304
- Skrutskie, M., Cutri, R. M., Stiening, R., et al. 2006, *AJ*, 131, 1163
- Taylor, M. B. 2005, *Astronomical Data Analysis Software and Systems XIV* (ASP Conf. Ser. 347), ed. P. Shopbell, M. Britton, & R. Ebert (San Francisco, CA: ASP), 29
- Taylor, M. B. 2006, *Astronomical Data Analysis Software and Systems XV* (ASP Conf. Ser. 351), ed. C. Gabriel et al. (San Francisco, CA: ASP), 666
- van Biesbroeck, G. 1944, *AJ*, 51, 61
- Voûte, J. 1917, *MNRAS*, 77, 650
- Wolf, M. 1919, *Veröffentlichungen der Badischen Sternwarte zu Heidelberg*, 7, 195
- Wright, E. L., Eisenhardt, P. R. M., Mainzer, A. K., et al. 2010, *AJ*, 140, 1868
- York, D. G., Adelman, J., Anderson, J. E., et al. 2000, *AJ*, 120, 1579

TABLE 1  
ASTROMETRY FOR WISE J104915.57–531906.1

$\alpha$ (J2000) ( $^{\circ}$ )	$\delta$ (J2000) ( $^{\circ}$ )	$\sigma_{\alpha,\delta}$ ( $''$ )	MJD	Source
162.355972	−53.321606	0.40	43617.5	DSS IR
162.338312	−53.320242	0.30	48690.6	DSS red
162.329376	−53.319612	0.08	51220.8	DENIS
162.328814	−53.319466	0.06	51315.1	2MASS
162.315519	−53.318500	0.07	55205.3	<i>WISE</i>
162.314540	−53.318283	0.07	55379.3	<i>WISE</i>
162.314283	−53.318415	0.12	55567.3	<i>WISE</i>

TABLE 2  
PARALLAX, PROPER MOTION, AND PHOTOMETRY FOR WISE J104915.57–531906.1

Parameter	Value
$\pi$	$0.496 \pm 0.037''$
$\mu_{\alpha} \cos \delta$	$-2.759 \pm 0.006'' \text{ yr}^{-1}$
$\mu_{\delta}$	$+0.354 \pm 0.006'' \text{ yr}^{-1}$
DENIS $i$	$14.94 \pm 0.03$
DENIS $J$	$10.68 \pm 0.05$
DENIS $K_s$	$8.87 \pm 0.08$
2MASS $J$	$10.73 \pm 0.03$
2MASS $H$	$9.56 \pm 0.03$
2MASS $K_s$	$8.84 \pm 0.02$
$W1$	$7.89 \pm 0.02$
$W2$	$7.33 \pm 0.02$
$W3$	$6.20 \pm 0.02$
$W4$	$5.95 \pm 0.04$

NOTE. —  $\pi$  and  $\mu$  were derived from a fit to astrometry from DSS, DENIS, 2MASS, and WISE (Section 3.2). The photometry is from the Third DENIS Release (DENIS J104919.0–531910), the 2MASS Point Source Catalog (2MASS J10491891–5319100), and the *WISE* All-Sky Source Catalog.

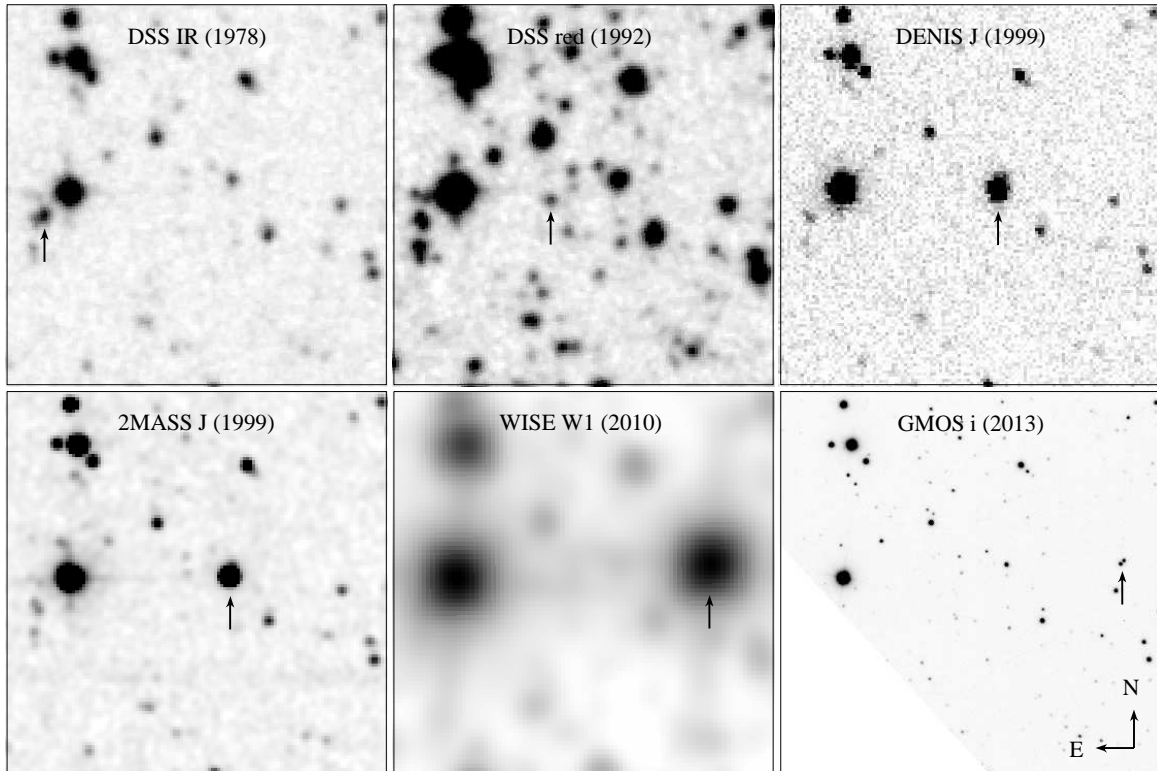


FIG. 1.— Detections of WISE 1049-5319 in images from DSS, 2MASS, DENIS, *WISE*, and GMOS (arrows). It is resolved as a  $1''.5$  binary by GMOS. The size of each image is  $2' \times 2'$ .

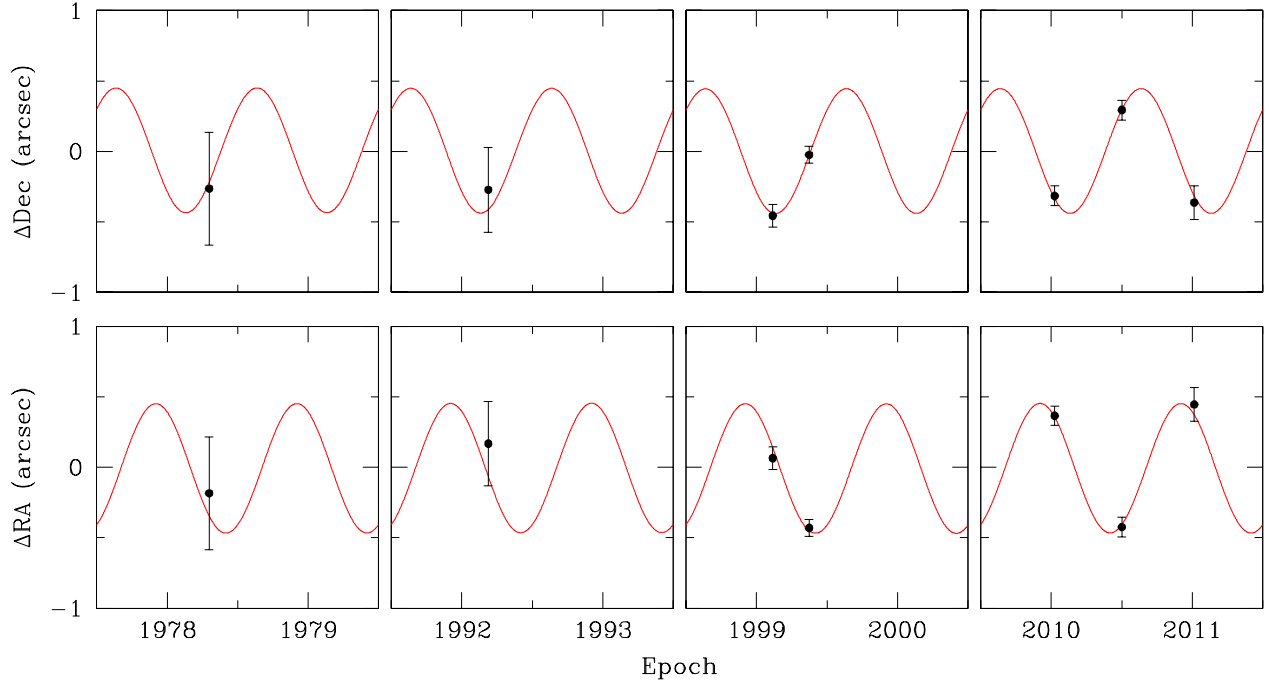


FIG. 2.— Relative astrometry of WISE 1049-5319 in images from DSS, DENIS, 2MASS, and *WISE* (points) compared to the best-fit model of parallactic motion (Table 2, red curve). The proper motion produced by the fitting has been subtracted.

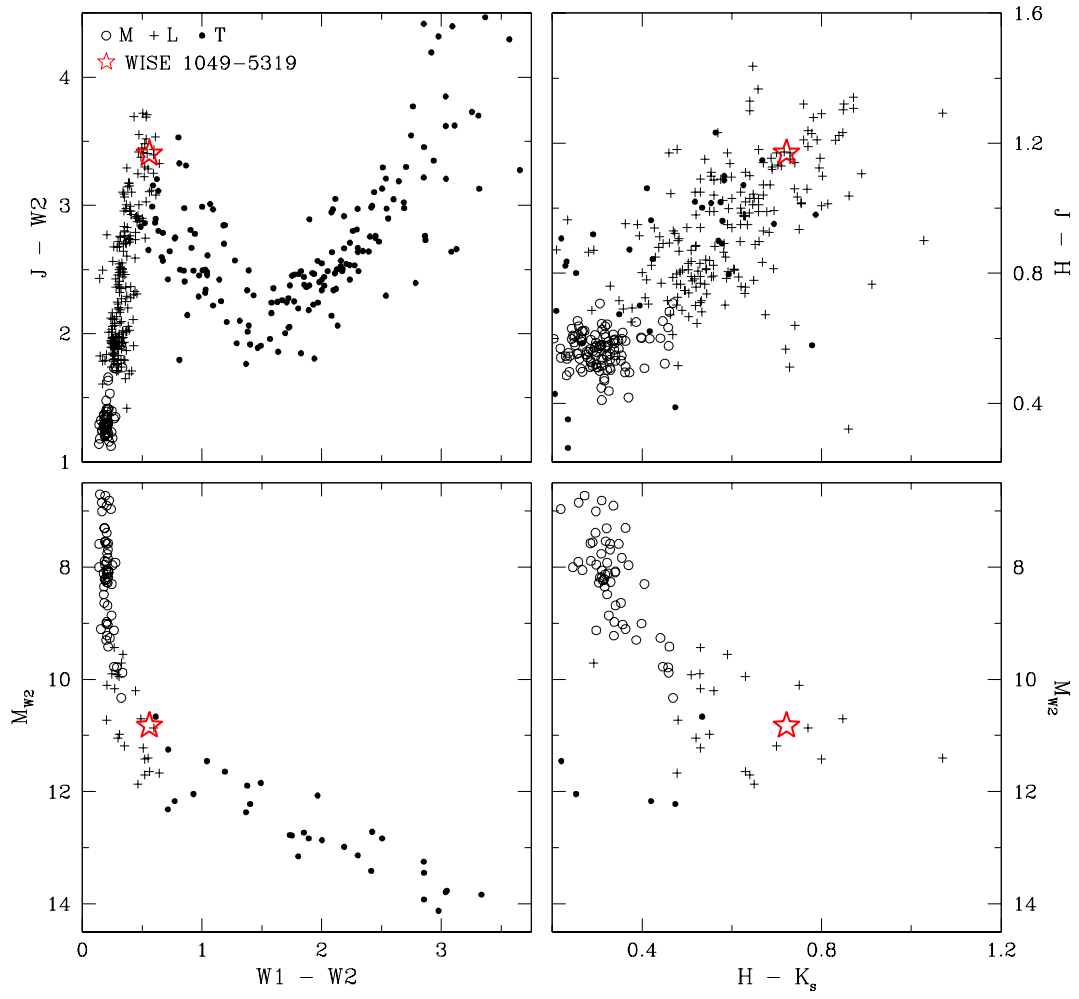


FIG. 3.— Color-magnitude and color-color diagrams for WISE 1049-5319 (star) and a sample of M, L, and T dwarfs (open circles, crosses, and filled circles, Leggett et al. 2010; Kirkpatrick et al. 2011, 2012, <http://DwarfArchives.org>).



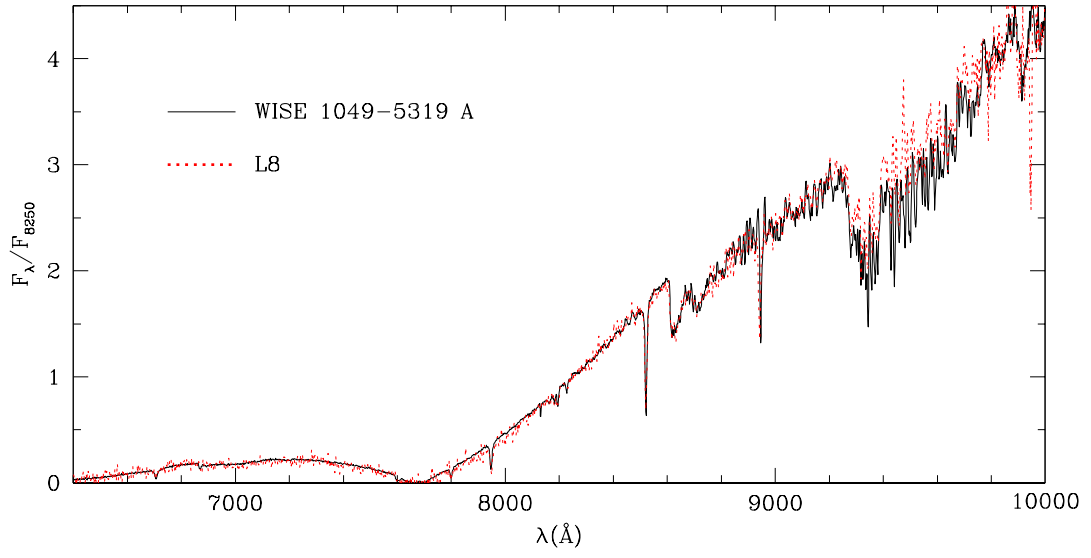


FIG. 4.— Optical spectrum of WISE 1049-5319 A compared to the L8 standard 2MASS J16322911+1904407 (Kirkpatrick et al. 1999).